Materials Research Proceedings 28 (2023) 621-628 https://doi.org/10.21741/9781644902479-67

Determination of recrystallisation phenomenon in type 316 stainless steel VIM-VAR ingots during cogging operations

PAQUETTE Arthur[1,a], LANGLOIS Laurent[2,b *], VIOLATOS Ioannis[1,c], RAHIMI Salaheddin[1,d], DUMONT Christian[3,e] and BIGOT Régis[2,f]

[1]Advanced Forming Research Center (AFRC), University of Strathclyde, 85 Inchinnan Drive, Inchinnan, Renfrewshire, PA4 9LJ, United Kingdom

[2]Arts et Métiers Institute of Technology, Université de Lorraine, ESAM Université, LCFC, 4 rue Augustin Fresnel, E-57070, France

[3]Aubert et Duval, Usine des Ancizes, Les Ancizes, 63770, France

[a]arthur.paquette@strath.ac.uk, [b]laurent.langlois@ensam.eu, [c]ioannis.violatos@strath.ac.uk, [d]salah.rahimi@strath.ac.uk, [e]christian.dumont@eramet.com, [f]regis.bigot@ensam.eu

Keywords: Cogging, Simulation, Recrystallisation, Stainless Steel, Ingot-To-Billet Conversion Process

Abstract. This study is focused on understanding the effects of key process parameters on the onset of recrystallisation of coarse, elongated, and dendritic grains of the as-cast microstructure during ingot-to-billet conversion, consisting of successive cogging, upsetting, and reheating operations, in type 316 austenitic stainless steel. The microstructural characteristics of the initial as-cast ingot (e.g., size, orientation and morphology of grains), and the complex thermo-mechanical path have significant impact on recrystallisation behaviours, which make the existing material models inefficient of precise microstructure prediction. These investigations aim at exploring the recrystallisation mechanisms and their dependency on the forging process parameters. Cogging trails were conducted on VIM-VAR stainless steel ingots and microstructural observations were made to identify the recrystallisation mechanisms. Finite element simulations coupled with constitutive material models were developed in parallel, to enable microstructurally informed prediction of the cogging process. Thus, static and discontinuous dynamic recrystallisations occur in succession after reaching a threshold level of deformation during cogging. Grain growth occurred in the statically recrystallised grains during reheating. The importance of the reheating and the associated static recrystallisation on the efficiency of the billet conversion process in terms of grain refinement is thus highlighted.

Introduction

The ingot-to-billet conversion process, consisting of hot forging operations of cogging and upsetting with intermediate reheating, is typically performed to generate a homogeneous and equiaxed grain microstructure from the initial as-cast's coarse, elongated, and dendritic structure. The different steps of the conversion route cause the occurrence of several metallurgical mechanisms, which lead to the evolution of microstructure. Continuous (CDRX) or Discontinuous (DDRX) dynamic recrystallisation are the main mechanisms of microstructure evolution, occurring during the hot forming operation. The plastic strain, strain rate and the temperature are the main thermomechanical parameters governing these mechanisms [1]. During intermediate reheating (i.e., between cogging/upsetting operations), static recrystallisation (SRX) can occur depending on the temperature and the accumulated strain energy in form of geometrically necessary dislocation density produced during the previous forming operations. Further, grain growth can also occur when the material is held at high temperatures for a long time, in particular, during heating and reheating processes.

Materials Research Proceedings 28 (2023) 621-628 https://doi.org/10.21741/9781644902479-67

The occurrence of these mechanisms are well-known in the case of austenitic stainless steels with an initial fine and equiaxed grain structure [1]. With the aim of optimising a forging route, the grain size can be predicted by Finite Element (FE) simulation integrating materials models, like the JMAK model [2], or full field models with scale transition [3].
However, the microstructural characteristics of the initial as-cast ingot have a significant impact on recrystallisation behaviours, which make the existing material models inefficient of predicting microstructure evolutions to a reasonable accuracy. For instance, the crystallographic texture resulting from the oriented solidification of the material during its casting, confers to the material an anisotropic plastic behaviour as described for type 718 nickel alloy by [4].

The present work aims at understanding the recrystallisation mechanisms in the as-cast microstructure occurring during ingot-to-billet conversion process of type 316 stainless steel. These involve investigating the effect of heating and thermomechanical processing on the evolution microstructure in the as-cast material with a coarse, elongated and dendritic grain microstructure. For this purpose, cogging trials were carried out following a typical industrial forging route, including intermediate heating. A FE simulation of the process was also conducted in parallel to estimate the evolution of stress, strain and temperature throughout the whole process. The experimental details are presented in a first part, and the second part is devoted to the numerical modelling of the cogging process. Finally, experimental and numerical results are presented and discussed.

Experiments

The initial ingot was a cylinder with a diameter of 190mm and a length of 600 mm (Fig. 1a). It was manufactured through a consecutive vacuum induction melting (VIM) and vacuum arc re-melting (VAR) processes. The as-cast macrostructure, similar to that reported by Park et al. for nickel superalloys [5], consisted of coarse dendritic grains elongated according to the solidification direction, oriented at ≈ 60° upwards with respect to the axis of the ingot (Fig. 1b), except in the centre, where the grains had their long axis parallel to that of the ingot.

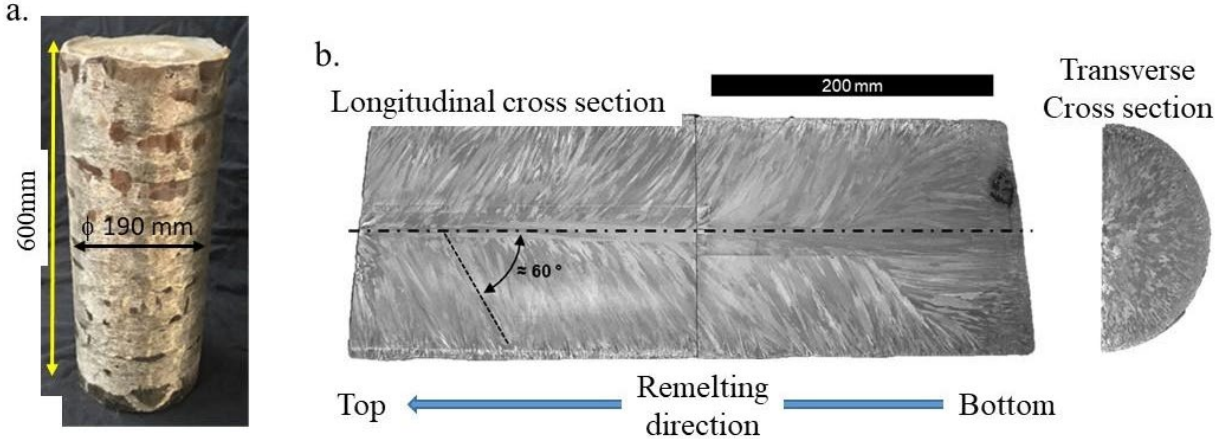

Fig. 1. Initial VIM/VAR melted type 316 austenitic stainless steel ingot, (a) a photograph of the ingot after being ground for the removal of surface scales, and (b) optical microscopy appearances of the longitudinal and transverse cross-sections of the ingot exhibiting the coarse, elongated, and dendritic grains, oriented at ≈ 60° to the axis of the billet.

The heating and cogging route is schematically depicted in Fig. 2. It consisted of three section-reduction stages of 20 %, 12 % and 12 % respectively, after an initial 12 h soaking at 1250°C, followed by two additional cogging stages of 20 % section-reduction after an intermediate 90 min reheating at 1250°C.

To investigate the effect of the different steps of the cogging route on the grain structure, and to highlight the occurrence of the different recrystallisation mechanisms, two ingots were forged. An ingot was subjected to the first three section-reduction stages before cooling to room temperature. The second was cogged according to the complete route presented in Fig 2, but the last two section-reduction stages were applied on its half-length only. Each section-reduction stage consisted of two successive cogging passes with an intermediate 90° rotation of the ingot (i.e., change of forging direction). Each cogging pass consisted of blows with an advancing feed of the ingot between two successive blows. The advancing feed of each stage and the target section dimensions are given in Table 1.

Table 1. Target section dimensions and feed of each stage (dimensions in mm).

Forging stage	1st	2nd	3rd	4th	5th
Target dimensions (mm²)	170 × 170	160 × 160	150 × 150	135 × 135	120 × 120
Feed (1st blow) (mm)	110	80	80	60	60
Feed (following blows) (mm)	60	30	30	30	30

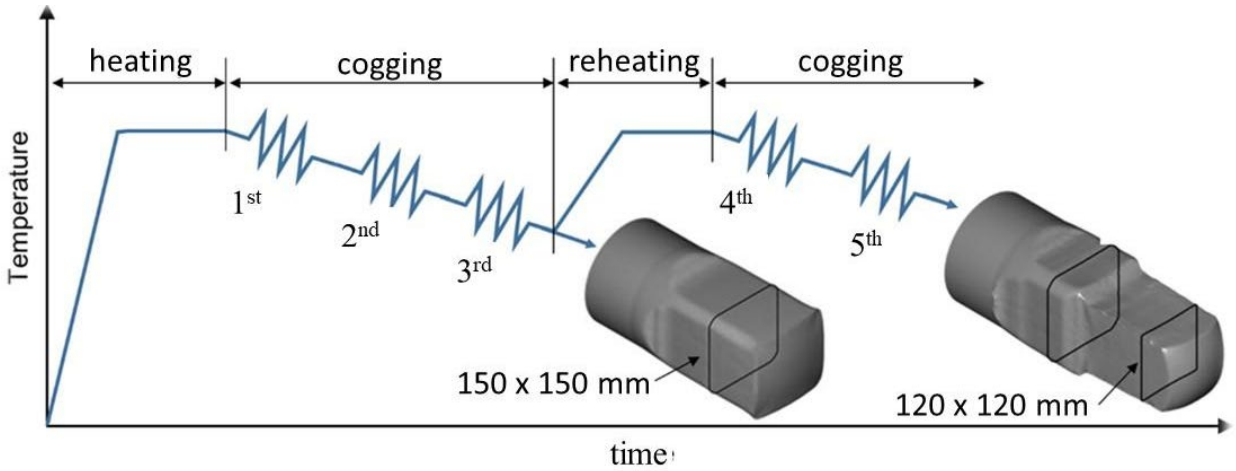

Fig. 2. Schematic illustration of the cogging route on the as-cast ingots.

The heating and reheating were performed in an electric furnace. The cogging operation were carried out using a LASCO® SPR-400 screw press. The ingots were initially coated with a refractory material to reduce oxidation during heat treatment and to limit heat losses during transfer from the furnace to the press. The ingots were handled by a six-axis robot equipped with a gripper (Fig. 3a and c), with unlockable compliances accommodating the axial and vertical deformation of the ingots during cogging blows. The anvils, whose main dimensions are given in Fig. 3b, were pre-heated to 450°C using embedded heating cartridges. Stoppers were placed between the upper and lower anvils to control the stroke.

After cogging, the ingots were optically scanned using a ATOS III Scan GOM® system. The ingots were then cut, ground and chemically etched to obtain optical macrographs from their longitudinal cross-sections. Smaller specimens were also machined out for further analyses at higher magnification by optical microscopy.

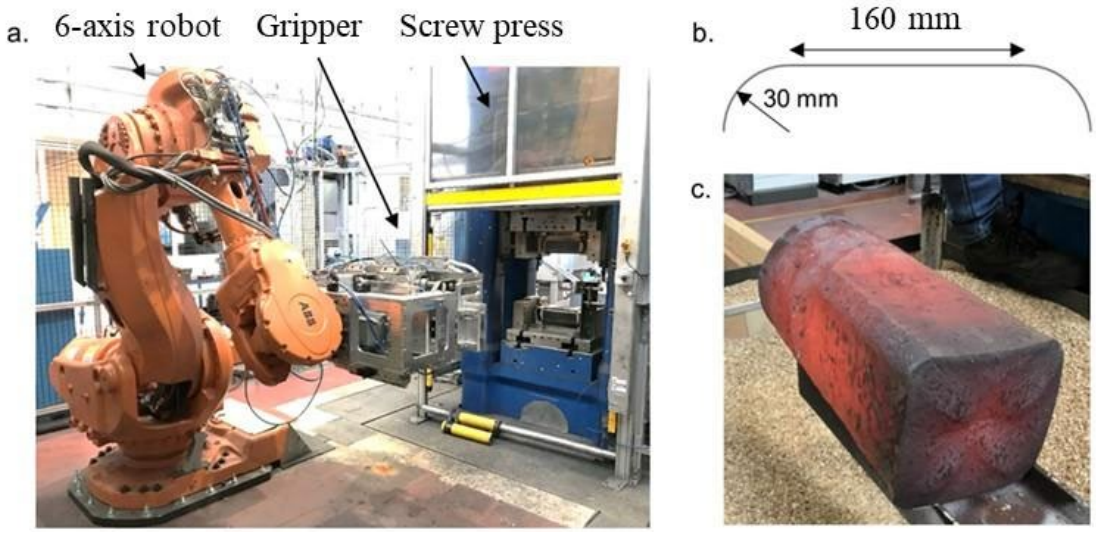

Fig. 3. (a) Experimental set-up, (b) the anvil profile, and (c) photographs of the ingot after the first three stages of the cogging operations.

Modelling and Simulation

The FE simulations were performed using the commercial Forge NxT 3.0® software to predict the evolution of temperature, plastic strain and strain rate within the ingot throughout the cogging route. A simplified Hensel-Spittel viscoplastic constitutive law was implemented into the FE model for the material's thermomechanical behaviour (Eq. 1). The material properties data for 316L were taken from the Forge® database.

$$\sigma = A \cdot e^{m_1 T} \cdot \varepsilon^{m_2} \cdot \dot{\varepsilon}^{m_3} \cdot e^{\frac{m_4}{\varepsilon}} \quad (1)$$

As shown by Paquette et al. [6], the anisotropy of the solidification induced textured microstructure was considered using the orthotropic Hill-48 criterion (Eq. 2). The constitutive law and the Hill criterion parameters are given in Table 2.

$$\sigma_0{}^2 = F \cdot (\sigma_{22} - \sigma_{33})^2 + G \cdot (\sigma_{11} - \sigma_{33})^2 + H \cdot (\sigma_{11} - \sigma_{22})^2 + 2L \cdot \sigma_{23}{}^2 + 2M \cdot \sigma_{13}{}^2 + 2N \cdot \sigma_{12}{}^2 \quad (2)$$

The Hill criterion was expressed in an anisotropic reference frame, assuming a grain orientation similar to that of the as-cast material (i.e., the solidification structure). In Eq. 2, the index 3 corresponds to the direction of solidification. The orientation of the anisotropic frame is symmetrically distributed around the axis of the ingot; hence the index 3 direction being orientated at 60° with respect to the axis of the ingot. The central zone of the ingot with the axially elongated grains was not taken into account.

Table 2. Hensel Spittel constitutive law parameters and orthotropic Hill-48 criterion parameters.

Hensel Spittel	A	m1	m2	m3	m4
	8905.34	-0.00383	0.01246	0.09912	-0.02413

Orthotropic Hill-48 criterion	F	G	H	L	M	N
	0.5	0.5	0.5	0.68	0.68	1.5

A Tresca limited Coulomb law ($\underline{m} = 0.4$, $\mu = 0.8$) was implemented to simulate the friction behaviour between the material and the anvil. The heat exchange rate between the ingot and the ambient medium was set to 10 $Wm^{-2}K^{-1}$, and to 10^4 $Wm^{-2}K^{-1}$ for the exchange with the anvils. The temperature of the anvil was set to 450 °C to make it similar to that of the experiments. According to the symmetries of the problem, the ingot was modelled by a quarter of the cylinder, with two planes of symmetry implemented (see Fig. 4). The ingot was meshed with tetrahedral elements with an average size of about 6.5 mm. The dies were considered as rigid bodies and their surfaces were meshed with triangular elements of 15 mm average size.

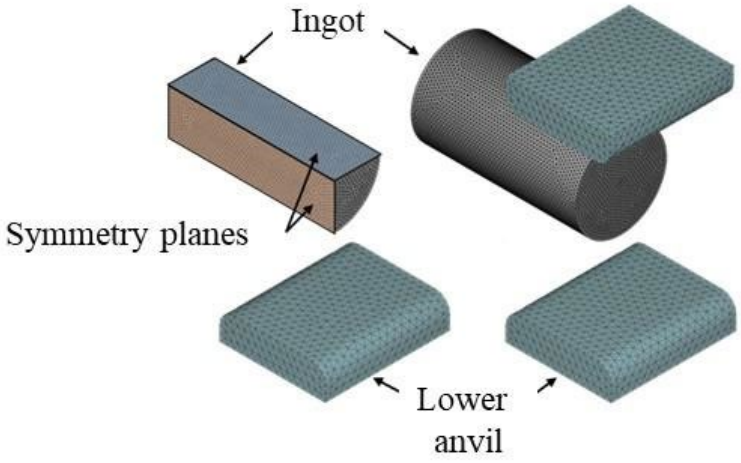

Fig. 4. Numerical model of the cogging operations.

A particular attention was paid to the temperature prediction, as it is one of the most influential thermomechanical parameters driving the recrystallisation mechanisms. The duration of each step of the cogging route, recorded during the trial, including the transfer from the furnace to the press, and the position of the ingot before each blow were therefore implemented in the simulation.

Results and Discussion

In Fig. 5, the 3D scan of the ingot after the first three stages of cogging and the simulated geometry obtained with both orthotropic and isotropic criteria are shown. It can be seen that the end of the ingot exhibited lobes along the diagonals. This feature was not captured by the FE simulation with the isotropic criterion implemented. On the other hand, the FE simulation with the anisotropic material model implemented allowed to predict the formation of these features, suggesting the important role of the anisotropy on the deformation behaviour of the as-cast material during the forging process. The geometrical discrepancy between the experimental and FE predicted geometries of the cogged ingot are highlighted by the circles in Fig. 5, and can partially be ascribed to the fact that the specific orientation of the grain at the centre of the ingot was not taken into account in the FE model.

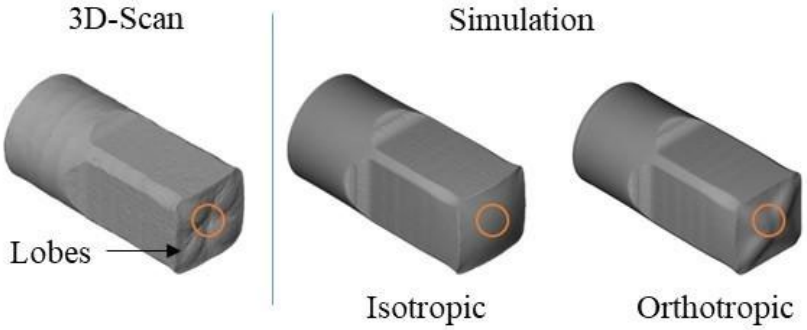

Fig. 5. Geometry of the ingot after the first three cogging stages; 3D scan after cogging trials, and FE simulated with isotropic and anisotropic material behaviours.

Fig. 6 presents macrographs of the two ingots. The macrograph of the first ingot (Fig. 6a) shows the macrostructure obtained at the end of the first three cogging stages, before the reheating. No obvious occurrence of recrystallisation can be seen from this macrograph.

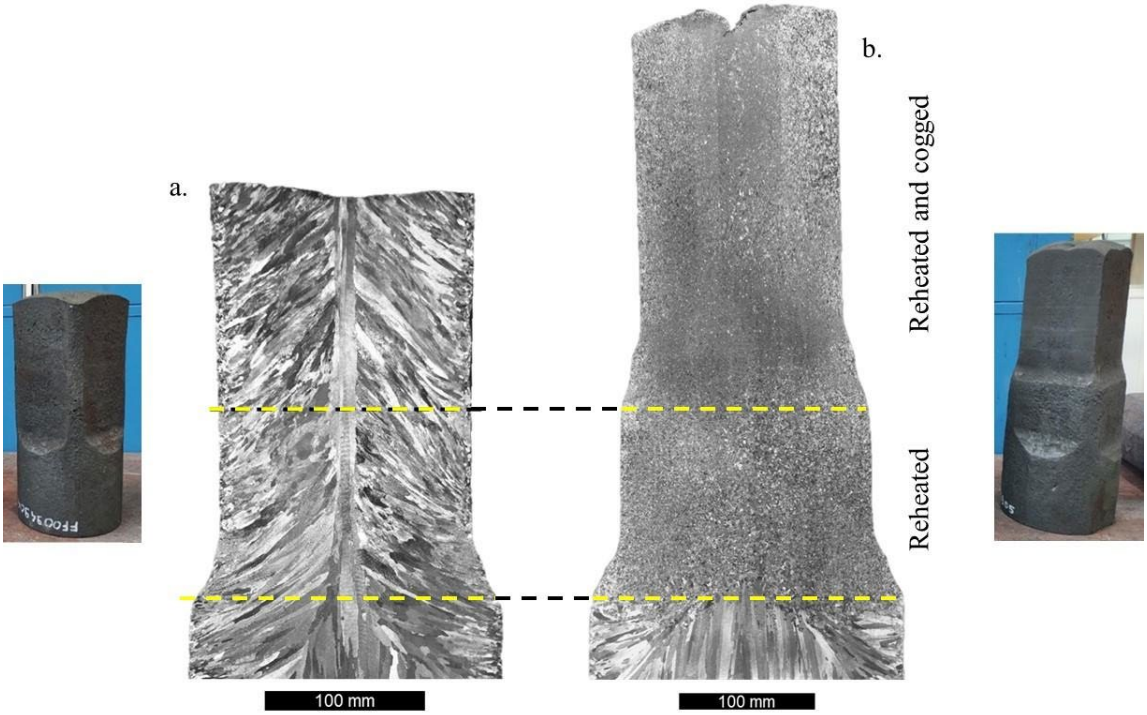

Fig. 6. Optical macrographs taken from the longitudinal cross-sections of the cogged ingots, (a) after the first three stages of cogging, and (b) following the complete cogging route plus reheating.

The macrograph of the second ingot can be split into two zones, (i) a reheated zone (RZ) which was re-heated after being cogged through the first three stages, and (ii) a reheated and cogged zone (RCZ) which was subjected to the complete cogging route. The onset of recrystallisation in both RZ and RCZ can clearly be seen in Fig. 6b. The difference in grain structure between the first ingot and the RZ is in the reheating, which has resulted in SRX of the material deformed during the first three cogging stages.

Analyses of higher magnification micrographs taken from different areas of these ingots were carried out to identify the recrystallisation mechanisms occurring during the cogging process (Fig. 7). Fig. 7a displays the microstructure in the cogged zone of the first ingot, where DDRX was observed at some boundaries of the parent microstructure. In the RZ of the second ingot, the recrystallised grains were large, but equiaxed. This confirms the occurrence of SRX, promoted by the deformation of the initial microstructure, induced by cogging. DDRX was very limited during the first cogging stages, and the plastic deformation was accommodated by strain hardening. SRX occurred during the reheating, and was followed by grain growth. In the RCZ, necklace type DDRX was observed. Such necklace-type DRX was previously reported in the literature for as-cast microstructures composed of large and elongated grains [6].

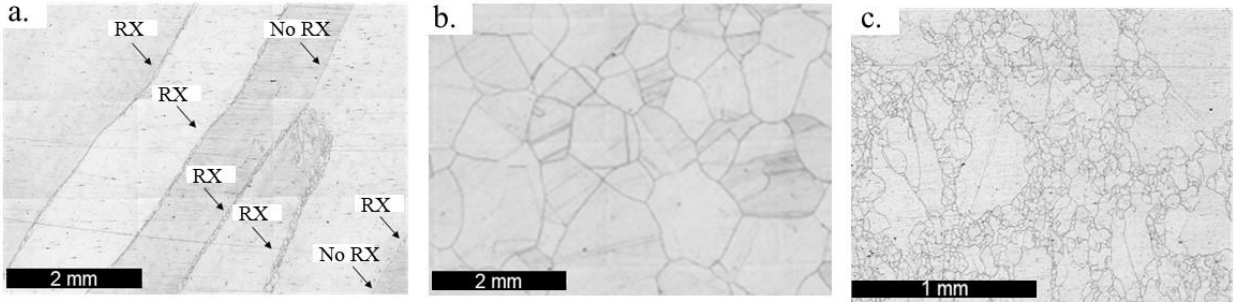

Fig. 7. Optical micrographs of the billets after cogging operations;(a) the cogged zone of the first ingot, (b) the reheated zone, and (c) the reheated and cogged zone of the second ingot.

Evolution of plastic strain and temperature during the first three cogging stages were estimated by FE simulation (Fig. 8). The maximum predicted strain was at the extremity of the ingot and was ascribed to the formation of the particular feature described in Fig. 5, as an edge effect. The final temperature at the core of the ingot was between 900 °C and 1000 °C, which are relatively low for DRX; and can explain the occurrence of strain hardening in the cogged zone of the first ingot.

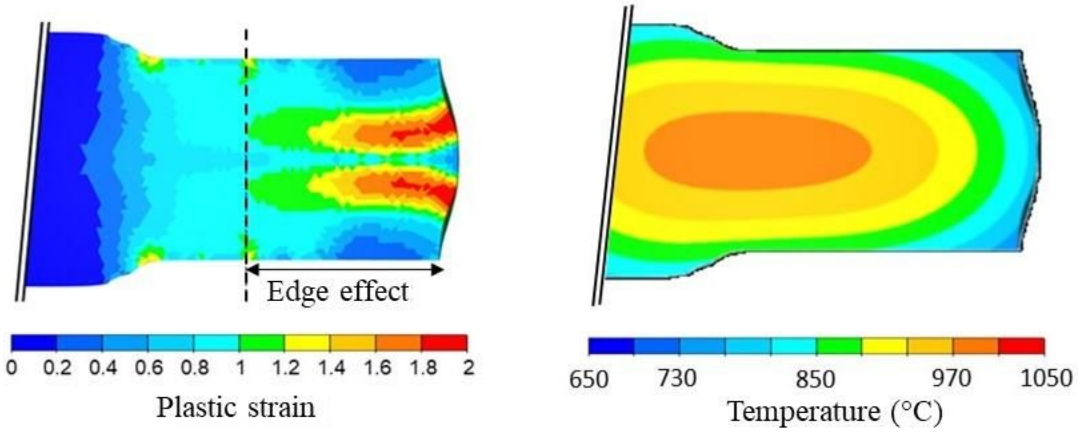

Fig. 8. Distributions of plastic strain and temperature predicted by FE simulations along the longitudinal cross-section of the ingot after the first three cogging stages.

Comparison of FE results and microstructures provided in Fig. 6 and Fig. 8, respectively, allowed to identify that SRX occurred during the reheating in the areas where the plastic strain obtained at the end of the first cogging stage was higher than the threshold value of ≈ 0.2.

The validity of the implemented anisotropic material model for equiaxed and recrystallised microstructure, such as that observed in the RZ, is questionable since the crystallographic texture of the microstructure issued from SRX was not characterised, and the parameters proposed by Paquette et al. [6] may not remain suitable. The last two cogging stages were therefore not simulated.

Summary

Cogging trials of VIM-VAR processed 316 type stainless steel ingots have been performed to investigate the recrystallisation mechanisms of an as-cast microstructure containing coarse, elongated, and dendritic grains. The cogging operations led to an insignificant amount of DDRX, localised to grain boundaries primarily. Otherwise, the cogging induced deformation led to strain

hardening during the initial stages of cogging, resulting in a significant level of static recrystallisation during the follow-up reheating. The latter led to new coarse, but equiaxed grains which then underwent DDRX during the following cogging stages (i.e., creating necklace structure). The efficiency of the SRX was a function of temperature gradient between the last cogging stage and the follow-up reheating. The large equiaxed grains after the reheating were most likely generated by normal grain growth, following the static recrystallisation. This must have been promoted by the higher temperature and the holding time of the reheating.

The strain hardening induced during the cogging process typically results from a competition between dislocations generation, their dynamic recovery, and the dynamic recrystallisation. The latter phenomena being favoured by a high temperature, as the lower the temperature at the end of the cogging stages the higher the strain hardening will become, and hence the more efficient the static recrystallisation during reheating. This study has shown the importance of temperature control and the role of static recrystallisation, as important parameters in optimising ingot-to-billet conversion processes.

Acknowledgement
The authors also would like to thank Alexandre Fendler for his technical contribution during the experiments. The authors express their thanks to ISEETECH for the provision of the VULCAIN Platform facilities.

References

[1] R.D. Doherty, D.A. Hughes, F.J. Humphreys, J.J. Jonas, D. Juul Jensen, M.E. Kassner, W.E. King, T.R. McNelley, H.J. McQueen, A.D. Rollett, Current issues in recrystallization: A review, Mater. Sci. Eng. A 238 (1997) 219-274. https://doi.org/10.1016/S0921-5093(97)00424-3

[2] M. Fanfoni, M. Tomellini, The Johnson-Mehl-Avrami-Kolmogorov model: a brief review, Nuovo Cimento della Societa Italiana di Fisica D – Condensed Matter, Atomic, Molecular and Chemical Physics, Biophysics. 20 (1998) 1171-1182. https://doi.org/ 10.1007/BF03185527

[3] D.A. Ruiz Sarrazola, L. Maire, C. Moussa, N. Bozzolo, D. Pino Munoz, M. Bernacki, Full field modelling of dynamic recrystallization in a CPFEM context – Application to 304L steel, Comput. Mater. Sci. 184 (2020) 109892. https://doi.org/10.1016/j.commatsci.2020.109892

[4] J. Terhaar, J. Poppenhäger, D. Bokelmann, H. Schafstall, K. Kelkar, Considering the solidification structure of VAR ingots in the numerical simulation of the cogging process, 7th International Symposium on Superalloy 718 and Derivatives (2010) 65-77. https://doi.org/10.1002/9781118495223.ch4

[5] N.K. Park, J.T. Yeom, J.H. Kim, X.X. Cui, Characteristics of VIM/VAR-Processed Alloy 718 Ingot and the Evolution of Microstructure During Cogging, in: Superalloys 718, 625, 706 and Various Derivatives, Presented at the Superalloys TMS (2005) 253-260. https://doi.org/10.7449/2005/Superalloys_2005_253_260

[6] A. Paquette, S. Rahimi, I. Violatos, L. Langlois, C. Dumont, J. Blaizot, M. Rosochowska, R. Bigot, On the evolution of microstructure and mechanical properties of type 316 austenitic stainless steel during ingot to billet conversion process, ESAFFORM2021 (2021), https://doi.org/10/25518/esaform21.929